Statistical analysis of water drop impact on surfaces with variable wettability

C. Antonini*, A. Amirfazli†, and M. Marengo*
* Dipartimento di Ingegneria Industriale, Università degli Studi di Bergamo,
Viale Marconi 5, 24044 Dalmine (BG), Italy
† Department of Mechanical Engineering, University of Alberta,
Edmonton, AB, Canada, T6G 2G8

Abstract

A statistical analysis of the main physical parameters describing water single drop impacts on solid surfaces with different wettabilities is presented. Aim of the study is to investigate the role of wettability during drop impact, in terms of drop deformation (e.g. maximum spreading) and dynamics characteristic times. Various surfaces were used during tests, in order to cover a wide range of contact angles, from 45° to 165°. One hundred different impact conditions were analyzed (12 different impact velocity on 8 different surfaces); each test was repeated ten times to confirm repeatability (approximately 1000 impact images were analyzed). Results show that two different regimes for spreading can be identified: for moderate We numbers (25<We<150) wettability plays a role in terms of both drop maximum spreading and characteristic time, whereas for high We numbers (We>150) wettability plays a minor role.

Introduction

Recently, a great interest is arisen for industrial application of so-called *superhydrophobic* surfaces (SHS), i.e. water repellent surfaces, for their capability to promote water shedding from the surface. The application of these surfaces would be beneficial in many fields, such as fuel cells [1], air conditioning systems, and icing [2].

A wide number of studies in literature is dedicated to the investigation of single and multiple drop impact on solid surfaces (see [3] for a comprehensive review). Majority of studies, either experimental [4]-[6], numerical [7],[8] or theoretical [9],[10], mainly refer to surfaces with high wettability (referred to as hydrophilic, when liquid is water), for which the contact angle (CA) at the three phase line is lower than 90°. Works investigating contact angles higher than 120° are not so frequent [11]-[16]. Thus, results and models in literature do not necessarily apply to impacts on surfaces with very low wettability, such as SHS.

The influence of wettability was first highlighted in 1958 by Hartley and Brunskill [17], who showed the importance of wettability to obtain a rebound of the drops after impact onto leaves. They proposed an energy balance approach for the spreading lamella in which they accounted for wettability through the value of a static contact angle.

An interesting phenomenological approach to drop impact on SHS was recently given by Rioboo *et al.* [11]. The definition of a qualitative drop impact regime map was proposed, with four different outcomes identified: deposition, rebound, sticking or fragmentation. It was found that the deposition-rebound limit and the rebound-fragmentation limit depend on a critical We number, which is a function of two parameters: the average contact angle, defined as the average between advancing and receding contact angles, and the contact angle hysteresis (contact angle definitions are discussed in the next section).

Drop rebound time was studied by Quéré and co-workers [12]-[14]. It was found that, in the investigated We range (0.3<We<37) [12], drop rebound time on a SHS does not depend on impact speed, but only scales with drop mass: drop rebound time is proportional to $m^{1/2}$. Recently, Bartolo *et al.* [15] focused their attention on the retraction dynamics of water drops on Parafilm®, which has a receding contact angle equal to 80°. They identified two different regimes (capillary-inertial and capillary-viscous) for drop retraction dynamics. Threshold between two regimes was found to be Oh=0.02 for the specific tested surface. Recently, Li *et al.* [16] investigated the effect of surface texturing on the receding phase and thus drop contact time. Test performed on textured silicon surfaces decorated by square arrays of pillars with different geometries showed that surface texture has a direct effect on receding contact angle and thus modifies retraction dynamics.

Although some works in literature have already dealt with drop impact on SHS, scantly a single study has examined a wide range of wettabilities. In the present work, drop impact tests were performed at moderate and high We numbers on eight different surfaces, to cover a wide range of contact angles and provide a comprehensive statistical analysis of the role played by wettability during drop impact.

* Corresponding authors: carlo.antonini@unibg.it, marco.marengo@unibg.it

Measurement of surface wettability

An essential issue in understanding the role of surface wettability during liquid-solid interaction after drop impact is how wettability can be measured, i.e. which parameters should be used to quantitatively evaluate surface wettability. Most of the works in literature relies on the evaluation of the equilibrium contact angle, θ_e, e.g. in [18]-[20]. Equilibrium contact angle can be univocally measured for a sessile liquid drop on an ideal, smooth surface. However, the measurement of an equilibrium contact angle on a real surface is questionable, since metastable configurations are possible and different values of the contact angle can be measured. For this reason, two values of the contact angle are often measured and reported as a measure of wettability: the advancing, θ_A, and receding, θ_R, contact angles, which are measured on a horizontal surface while quasi-statically expanding and contracting a drop, respectively. The difference between the two values is referred to as contact angle hysteresis (CAH), and is often used as a reference parameter to measure drop mobility on a surface: the lower the contact angle, the higher the mobility and the easier the drop shedding. Other measurements of the contact angle can be given, e.g. maximum and minimum contact angle, $\theta_{\min}$ and $\theta_{\max}$, respectively, which are measured for a drop on a tilted surface [21] or a drop exposed to aerodynamic surfaces [22] at the moment of incipient motion. As a further consideration, drop impact is not a quasi-static process and different dynamic contact angles can be observed, depending on the impact conditions. Numerical simulation, which require values of contact angles to be specified as a boundary condition, often rely on the so-called Hoffman's law [23], which provides the value of the dynamic contact angle as a function of the equilibrium contact angle and the capillary number, $Ca = \mu V_{cl} / \sigma$, defined using the contact line velocity, V_{cl}. Although the original Hoffman's law was derived for hydrophilic surfaces only, the approach is still widely used as demonstrated by a recent study by Roisman *et al.* [24], who used a modified form of Hofmann's law and demonstrated good agreement between numerical simulation and experiments for low We numbers (0.9<We<8) for one specific case of $\theta_e = 120°$. However, the application of usual boundary conditions, such as the Hoffman's law for the dynamic contact angle and no-slip condition at the liquid-surface interface, do not necessarily apply to the case of drop impact on SHS [25].

Different methodologies to measure contact angles point out that the choice of one or more parameters to synthetically define wettability is not a trivial issue and care must be taken in correlating contact angles measured in quasi-static conditions to study strongly dynamic phenomena.

Methods and Materials

Drop impact tests were performed on the following surfaces: (i) smooth glass; (ii) PMMA; (iii) Teflon; (iv) SHS-Teflon; (v) OTSa; (vi) OTSb; (vii) OTSc; (viii) OTSd. Surface (ii) and (iii) were made by applying a coating on a smooth aluminum sample, whereas surface (iv) consist of a chemically etched aluminum sample, on which the same coating as on (iii) was applied (see [22] for complete description of surface (ii) to (iv) preparation). Surfaces (v) to (viii) were grafted with octadecyltrichlorosilane following the procedure described in details in [26], each exposed to UV for different times. All surfaces were characterised by measuring advancing (θ_A) and receding (θ_R) contact angles using the sessile drop method.

A typical test apparatus for drop impact studies was used, in which a drop is generated at the tip of a needle, then is accelerated by gravity and impacts normally on a surface. Images of drop impact were recorded using a high-speed camera (PCO 1200-hs) with a frame rate up to 21000fps and pixel resolution in the range 12-30μm (depending on magnification and required field of view). Figure 1 illustrates two image sequences for a drop impacting on PMMA and SHS-Teflon. Majority of images were recorded from side (horizontal camera positioning); few images were recorded mounting the camera with a tilt angle of 19° for those tests were the presence of secondary drops disturbed observation from side (typically on SHS at high We numbers). Images were automatically analyzed using a code, developed in MatLab® environment; the code can provide: (1) time evolution of contact diameter evolution, $D(t)$, and spread factor $\xi(t) = D(t) / D_0$; (2) maximum spread factor $\xi_{\max} = D_{\max} / D_0$; (3) drop final spread factor; (4) time to maximum spread factor $t_{\xi_{\max}}$; (5) time at maximum spread factor, $\Delta t_{\xi_{\max}}$, i.e. the time delay between the moment drop stops spreading and the moment drop starts receding; and eventually (5) drop rebound time, if drop rebounds. In order to calculate $t_{\xi_{\max}}$ and $\Delta t_{\xi_{\max}}$, the image analysis code calculates two times, t_s and t_r, which correspond to the time instants when drop stops spreading and when drop starts receding, respectively (see Figure 2). The two instants are identified as the two times when spreading ratio, ξ, crosses the threshold $0.99\xi_{\max}$. $t_{\xi_{\max}}$ is calculated as the average of t_s and t_r, and $\Delta t_{\xi_{\max}}$ as their difference (see Figure 2).

Drop diameter was kept constant (2.86mm±1%), velocity was varied from 0.83 to 4.16m/s (±0.6%), to give a constant Ohnesorge number (Oh=0.019±0.5%) and We numbers in the range 25 to 680 (±2.2%)

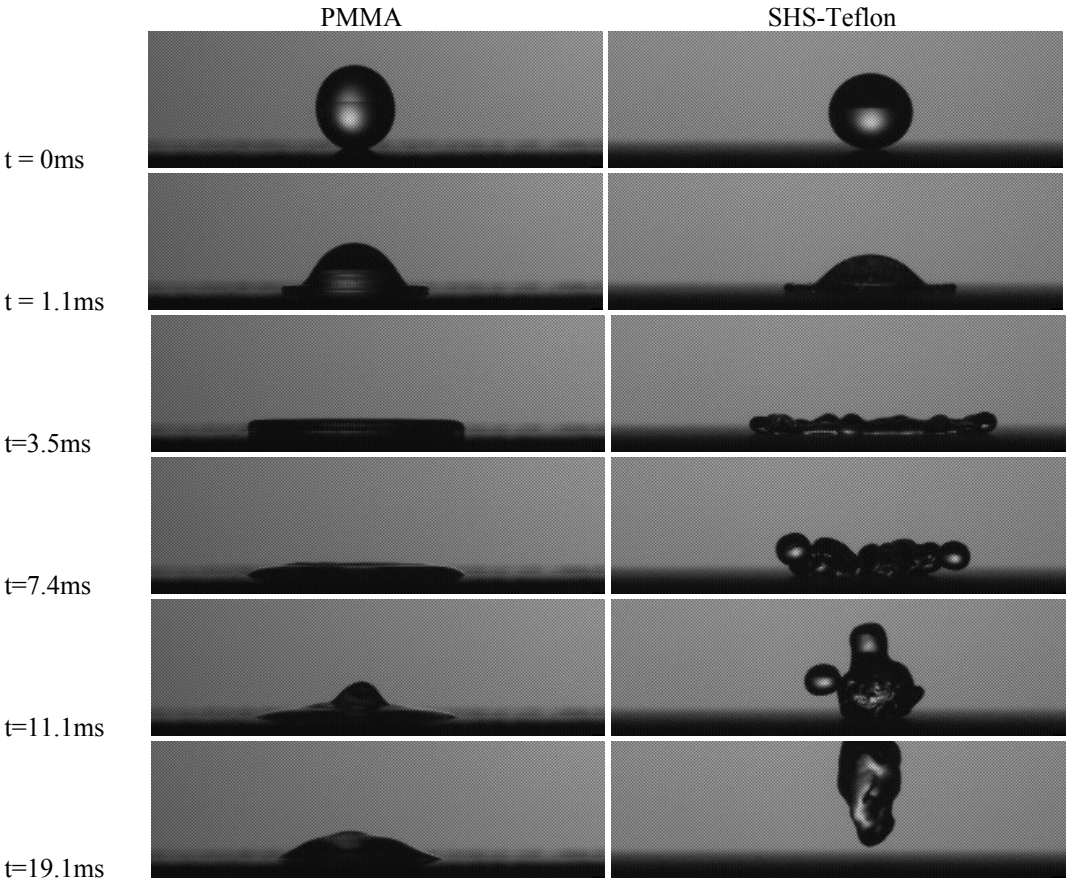

Figure 1: Image sequence of water drop impacting on a dry surface (D=2.86mm, V=1.36m/s, We=74, t_{conv}=D/V=2.1ms). Surfaces are PMMA (left column) and SHS-Teflon (right column). Water drop rebound can be observed on SHS-Teflon surface.

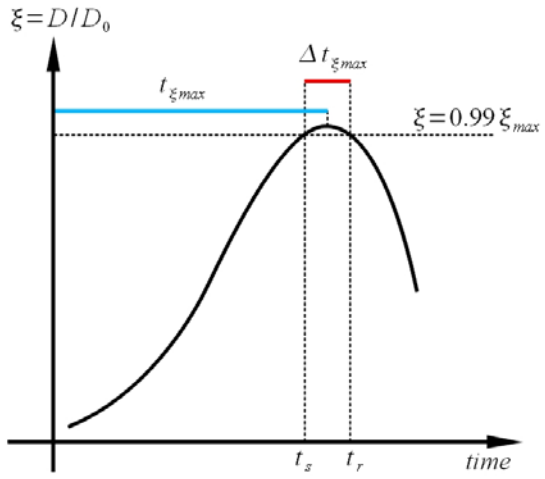

Figure 2: Schematic of spread factor evolution in time. Automatic image analysis code first detects t_s and t_r, identified as time when $\xi = 0.99\xi_{\max}$; $t_{\xi_{\max}}$ and $\Delta t_{\xi_{\max}}$ are calculated as their average and the difference, respectively. Axes are not scaled.

Table 1: Advancing (θ_A) and receding (θ_R) contact angles for all tested surfaces.

surface	glass	PMMA	Teflon	SHS-Teflon	OTSa	OTSb	OTSc	OTSd
θ_A [°]	46	88	113	162	112	99	55	68
θ_R [°]	<5	39	90	154	100	82	<10	35

Results and Discussion

Figure 3 shows that for moderate We (We=30), wettability significantly influences drop deformation during both spreading and receding phases: the lower the wettability, the lower the spreading and the spreading time (see Table 1 for wettability data). Differences in maximum spread factor are approximately 30% between most hydrophilic and most hydrophobic surfaces. Also, on the SHS-Teflon rebound of the drop is observed after receding phase, where drop contact diameter oscillates on the two other surfaces, until steady state is reached.

Figure 4a illustrates maximum spread factor trend as function of We for different surface wettabilities. Two regimes can be clearly identified: for moderate We number (25<We<150), drop spreading is influenced by surface wettability; for high We number (We>150) wettability plays minor role and all curves converge. Figure 4b allows a comparison between experimental data (glass, OTSa, SHS-Teflon) and mostly used correlations for predicting maximum spread factor; i.e. Scheller-Bousfield [4] and Roisman [10] for hydrophilic surfaces and Clanet *et al.* [13] for superhydrophobic surfaces. Scheller-Bousfield prediction fits well the experimental data in the high We regime, but overpredicts the spread factor in the moderate We regime. Roisman's correlation [10], which is a semi-empirical correlation derived using theoretical considerations and experimental data fitting, works very well for impacts on glass (most hydrophilic surface) in the entire We range. With regards to experimental data for SHS-Teflon, we observed a different trend from what observed by Clanet *et al.* (tests in the range (0.3<We<37), who found the drop spreading scaling with $We^{1/4}$ on a SHS: Clanet's correlation [13] does not fit our experimental data neither at moderate nor at high We number.

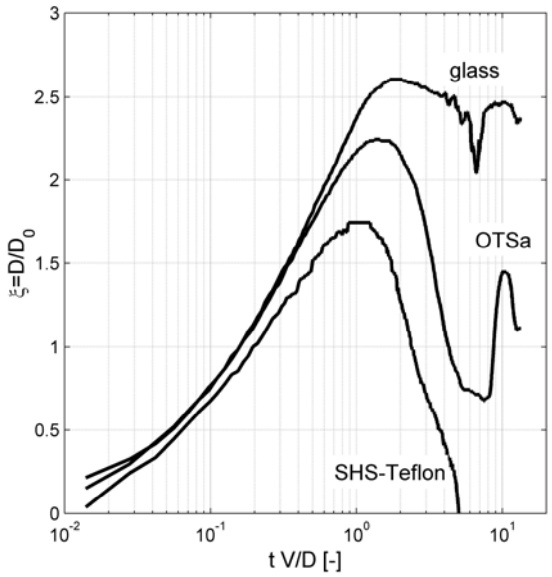

Figure 3: Spread factor, $\xi = D / D_0$, versus non-dimensional time for drop impact on surfaces with different wettability (We=30, Oh=0.019). Drop rebounds from surface on SHS-Teflon (when $\xi = 0$), whereas contact diameter D oscillates on glass and OTSa, until steady state is reached.

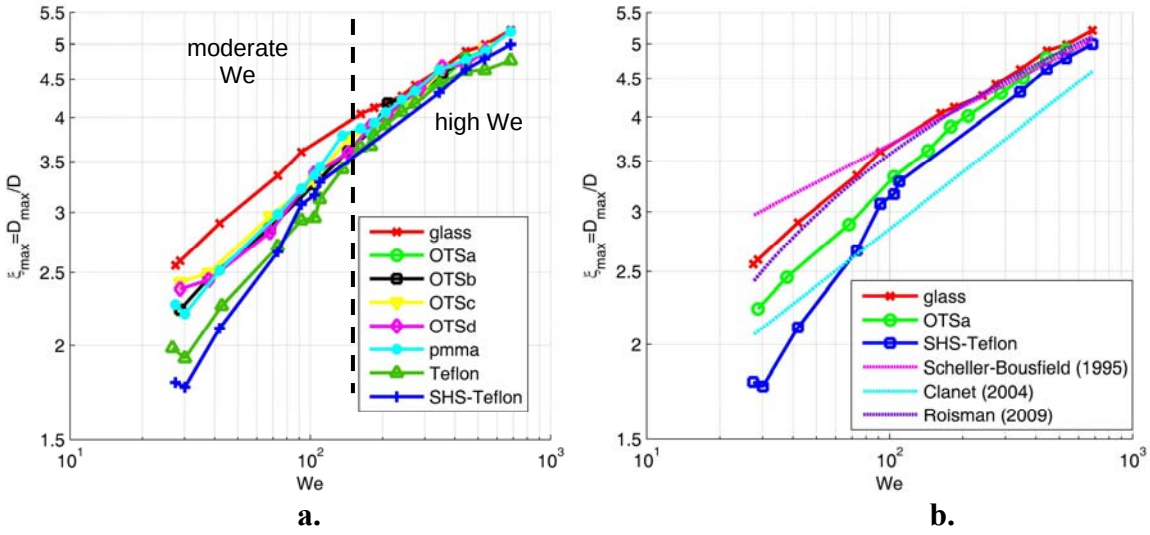

Figure 4. (a) Maximum spread factor versus We for drop impacts on surfaces with different wettability. (b) Comparison with correlations in literature for maximum spread factor: Scheller-Bousfield [4] $\xi_{\max} = 0.61\left(We/Oh\right)^{0.166}$; Roisman [10] $\xi_{\max} = 0.87Re^{1/5} - 0.40Re^{2/5}We^{-1/2}$; and Clanet [13] $\xi_{\max} = 0.9We^{1/4}$.

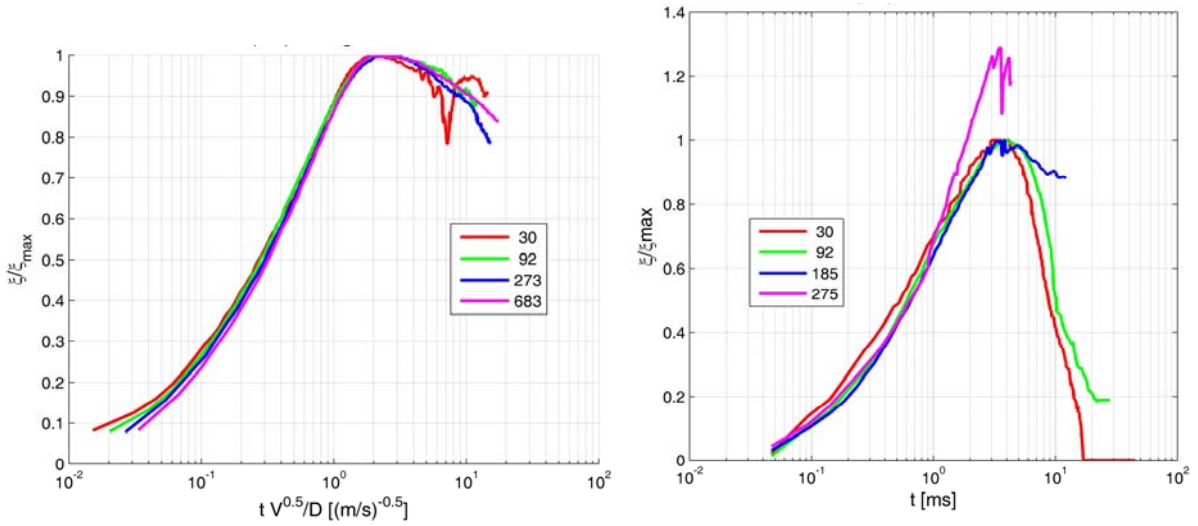

Figure 5. Drop spread factor, scaled by maximum spread factor, in time on glass (a) and on SHS-Teflon (b) at different We numbers (legend indicates the value of We). The value of drop spreading is scaled by the maximum drop spreading. Different time scales are used: (a) time is multiplied by $V^{0.5}/D$ (b) time in ms. Automatic image analysis was not performed for We>275 on SHS-Teflon due to drop fragmentation: presence of secondary drops ejected from the rim makes automatic image analysis impossible.

Very interesting outcomes are related to drop impact characteristic times. Figure 5a and Figure 5b illustrate the time evolution of the parameter $\xi/\xi_{\max}$ (which equals $D/D_{\max}$), on glass (see Figure 5a) and SHS-Teflon (see Figure 5b). Drop spreading evolution at different We is reported. For glass (see Figure 5a) all curves in the investigated range (30<We<683) collapse on a single curve if time is scaled with $V^{-1/2}$, suggesting that drop characteristic times most likely scales with $We^{-1/4}$. Note that all curves overlap well not only in the spreading, but also in the receding phase. Differently, on the SHS-Teflon (Figure 5b) all spreading curve collapse on a single curve with no scaling of time, i.e. drop spreading time does not depend on impact speed in the investigated range. Curve overlap quite well even in the receding phase, although this is not apparent from Figure 5b: automatic image analysis was complicated during the receding phase by presence of secondary drops (drop break-

up). Nevertheless, manual image analysis showed that drop evolution during receding phase is similar, as confirmed by the fact that drop rebound time is constant, as shown below. Note that data in Figure 5b refer to the range 30<We<257, because for higher We numbers drop break-up occurs in the final stage of the spreading phase and the image analysis code cannot measure drop spreading automatically. Indeed, the occurrence of break-up can be observed for the We=275 curve: drop remains united until $t = 1ms$ (when rim start deceleration), then break-up occurs and a secondary drop is ejected at high speed from the rim, as shown by the sudden change in drop spread factor derivative at $t = 1ms$.

The drop spreading time trend with We is well illustrated by Figure 6. For moderate We numbers, surface wettability has an effect on spreading time: at We=30, spreading time varies from 3.5ms for SHS-Teflon and 9ms for glass. On one hand, most hydrophilic surface, like glass, show a $We^{-1/4}$ trend, similar to the spreading time trend at higher We number. On the other hand, hydrophobic and superhydrophobic surfaces (i.e. OTSa, OTSb, Teflon, SHS-Teflon) show an almost constant spreading time. For high We numbers (We >150), spreading time mainly depends on impact We number and influence of wettability is reduced: curves from different surfaces tend to converge to a single line at higher We, the slope is $We^{-1/4}$. The only curve that is somewhat separated from others is the SHS-Teflon curve. However, differences are most likely attributable to significant drop break-up occurring at the end of spreading phase, causing alteration of drop spreading and also making identification of spreading time more difficult (tilted camera over the horizon was used and images were analyzed manually for impacts on SHS-Teflon at high We).

Another interesting characteristic time is the time at maximum spreading, $\Delta t_{\max}$, i.e. the time shift between the moment the drop stops spreading and when it starts receding. A clear trend of data can be observed: time at maximum spreading decreases with increasing We number and with increasing hydrophobicity. It is of note that for $\Delta t_{\max}$ distinction between moderate and high We numbers is not apparent as for drop spreading time: on a logarithmic scale, all curves from hydrophilic surfaces maintain the same slope ($We^{-2/5}$ for glass surface) and are almost parallel to each other on the entire analyzed We range. Surfaces with lowest wettability (SHS-Teflon, OTSa, OTSb) show approximately constant time at maximum spreading for moderate We. In particular, correlation between wettability and $\Delta t_{\max}$ can be found by looking at contact angle hysteresis, rather than advancing contact angle. For example, Teflon sample, which is less wettable than OTSa and OTSb (considering advancing contact angle), but has higher contact angle hysteresis, show a trend more similar to more hydrophilic surface, like PMMA, which has similar CAH. Trend for time at maximum spreading, $\Delta t_{\max}$, can be explained considering that when drop is at its maximum diameter, contact line speed is close to zero and capillary effect play indeed an important role, compared to convective effects. Also, at very low speeds (or more precisely at low capillary number, *Ca*), dynamic contact angles are close to the advancing and receding contact angles (measured in a quasi-static process): thus, advancing and receding values can be correlated to the time at maximum spreading, which is a characteristic time of an inertial event. The role of capillarity can be understood well looking back at Figure 3: in the first stages of spreading (until 3-4 convective times, D/V), glass and OTSa spread factor curves are overlapped, whereas in the later spreading stages, when rim decelerates down to zero velocity, wettability starts influencing drop dynamics evolution [6].

A further important characteristic time is drop rebound time, in case rebound occurs. Among all tested surfaces, complete rebound was observed only for SHS-Teflon surface. Partial rebound was observed on OTSa, OTSb and Teflon in the We range 40<We<200. Figure 7 illustrates rebound time for SHS-Teflon surface as function of impact speed. Rebound time is constant not only for lower impact speeds (corresponding to moderate We), but in the entire impact velocity range: rebound time is approximately 20.3ms. Data confirms qualitatively results from [14] (obtained for maximum impact velocity of 1.5m/s and We<40), in which it was found that drop rebound time is only a function of drop size and not impact velocity. In [14], the following correlation between drop rebound time and drop diameter was found:

$$t_{\text{rebound}} = 2.65\left(\frac{\rho D_0^3}{8\sigma}\right)^{1/2} \tag{1.1}$$

which predicts rebound time to be 16.9ms (for $D_0 = 2.86mm$), underestimating drop rebound time by approximately 20%. Since no details were provided in [14] on the exact value of the advancing and receding contact angles (it is only said on page 52 that observation were made on SHS, "that is, a micro-textured hydrophobic surface on which contact angles are typically of the order of 160°" [14]), we do not have enough information to argue whether differences should be attributed to different surface properties (e.g. contact angle values or surface texture) or shall be attributed to experimental uncertainties. Nevertheless, it is noteworthy that drop rebound time

remains constant even in the high We regime (We>150), though significant break-up of the drop occurs, especially during the receding phase.

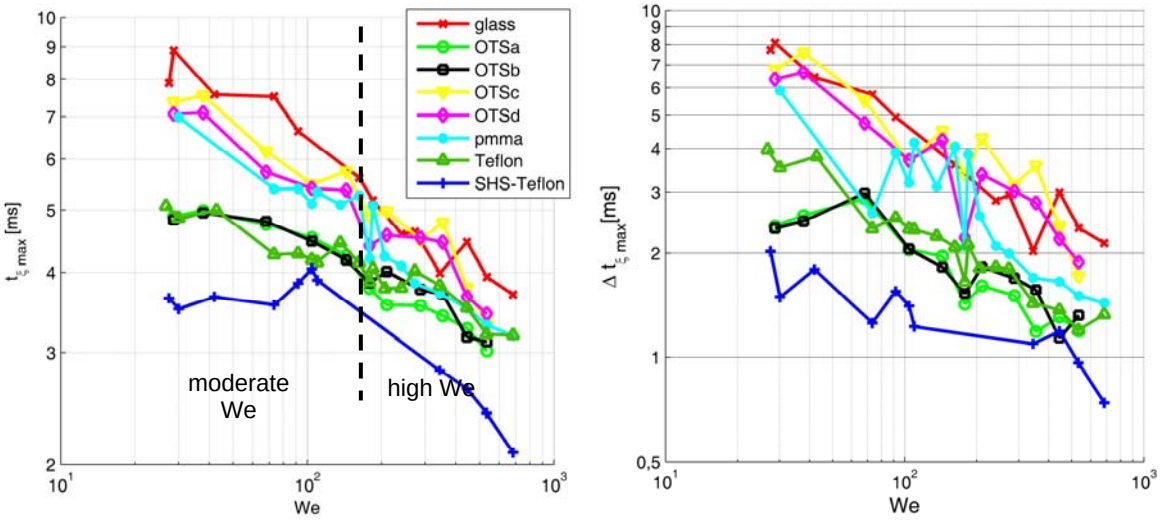

Figure 6. (a) Time to maximum spreading t_{max}. (b) Time at maximum spreading, Δt_{max} (see definition in section *Methods and Materials*).

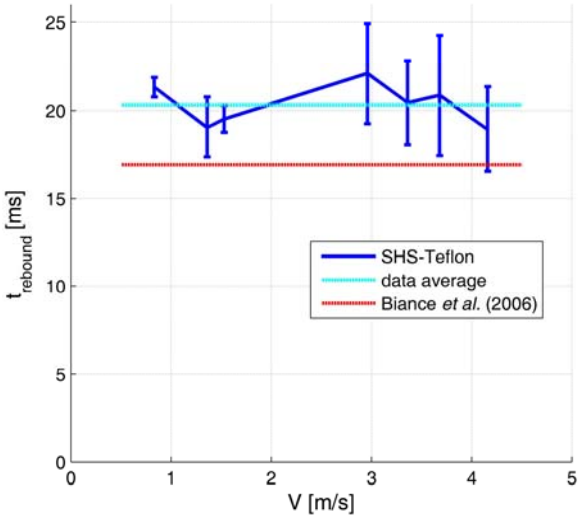

Figure 7. Rebound time vs. We number for drop impacts on SHS-Teflon. Data are compared to prediction from Biance *et al.* [14]. The corresponding range for the x-axis of in terms of We is 25<We<680.

Conclusions

Impact of millimetric water drops was studied or a large range of We number (25<We<680) for eight surfaces with different wettabilities. Results from impact image analysis have shown that two impact regimes can be identified for drop spreading. For moderate We numbers (30<We<150) drop spreading, i.e. maximum spreading and spreading time, are influenced by both impact conditions (We) and surface wettability. For high We numbers (We>150), forces are small compared to inertial forces and convection becomes predominant with respect to capillary effects: thus, drop spreading is mainly affected by We number and role of wettability is secondary.

Results on a hydrophilic surface show that curves of drop spread factor evolution collapse on one single curve if time is scaled by $V^{-1/2}$, suggesting that drop evolution characteristic time most likely scales with $We^{-1/4}$. Drop spreading on a SHS is qualitatively different, since characteristic time of drop evolution does not appear to be influenced by impact condition, in particular impact velocity, for moderate We numbers. Drop re-

bound time on SHS-Teflon was seen to be constant not only for low impact velocities (corresponding moderate We), but in the entire observed velocity range (up to 4.2m/s, corresponding to $We = 680$).

Acknowledgements

The authors acknowledge Alenia Aermacchi for interest and financial support. The authors acknowledge D. Barona (University of Alberta), R. Rioboo, S. Goosens and J. De Coninck (University of Mons) for surface preparation.

References

[1] A. Theodorakakos, T. Ous, M. Gavaises, J.M. Nouri, N. Nikolopoulos, H. Yanagihara, J. Colloid Interface Int. Sci. 300:673–687, 2006.
[2] M. Innocenti, C. Antonini, M. Marengo, A. Amirfazli. 13th IWAIS, Andermatt, Switzerland, Sept. 2009.
[3] A.L. Yarin, Annual Review of Fluid Mechanics 38:159–192, 2006.
[4] B. L. Scheller and D. W. Bousfield, AIChE J. 41, 1357-1367 (1995).
[5] Š. Šikalo, M.Marengo, C. Tropea, E.N. Ganić. Exp. Therm. Fluid Sci. 25, 7, pp. 503-510, 2002.
[6] R. Rioboo, M. Marengo, and C. Tropea. Exp. Fluids, 33(1):112–124, 2002.
[7] J. Fukai, Y. Shiiba, T. Yamamoto, O. Miyatake, D. Poulikakos, et al. Phys. Fluids 7:236–47, 1995.
[8] M. Pasandideh-Fard, S. Chandra, J. Mostaghimi, Int. J. Heat Mass Trans. 45:2229–42, 2002.
[9] I.V. Roisman, E. Berberović, C.Tropea. Phys. Fluids 21, 052103, 2009.
[10] I.V. Roisman. Phys. Fluids 21, 052104, 2009.
[11] R. Rioboo, M. Voué, A. Vaillant, and J. De Coninck. Langmuir, 24, 14074-14077, 2008.
[12] D. Richard, C. Clanet, D. Quéré, Nature 417, 811, 2002.
[13] C. Clanet, C. Béguin, D. Richard, D. Quéré. J. Fluid Mech., 517, 199–208, 2004.
[14] A.L. Biance, F. Chevy, C. Clanet, G. Lagubeau, D. Quéré. J. Fluid Mech., 5554, 47–66, 2006.
[15] D. Bartolo, C. Josserand, D. Bonn. J. Fluid Mech., 545, pp. 329–338 (2005).
[16] X. Li, X. Ma, Z. Lan. Langmuir, 26(7), pp. 4831–4838, 2010.
[17] G. Hartley, R. Brunskill. In: Surface Phenomena in Chemistry and Biology (ed. J. F. Danielli), 214–223. Pergamon, 1958.
[18] H.-Y. Kim and J.-H. Chun. Phys. Fluids 13, 3, 643-659, 2001.
[19] R. Bhola and S. Chandra. J. Matt. Sci., 34,19,4883– 4894, 1999.
[20] S.D. Aziz and S. Chandra. Int. J. Heat Mass Transfer, 43, 16, 2841-2857, 2000.
[21] E. Pierce; F.J. Carmona; A. Amirfazli. Colloids Surfaces, A 2008, 323, 73–82.
[22] A. J. B. Milne, A. Amirfazli, Langmuir, 25 (24):14155–14164, 2009.
[23] S.F. Kistler, Hydrodynamics of wetting, in: J.C. Berg (Ed.), Wettability, Marcel Dekker Inc., New York, 1993, pp. 311–429.
[24] I.V. Roisman, L. Opfer, C. Tropea, M. Raessi, J. Mostaghimi, S. Chandra. Colloids Surfaces A: Physicochem. Eng. Aspects 322 183–191, 2008.
[25] G. McHale, M.I. Newton, N.J. Shirtcliffe. Soft Matter, 6, pp. 714 – 719, 2010.
[26] R. Rioboo, M. Voue, H. Adao, J. Conti, A. Vaillant, D. Seveno, J. De Coninck, Langmuir, 26(7), 4873–4879, 2010.